The effect of pH on the fat and protein within cream cheese and their influence on textural and rheological properties

Lydia Ong[a,b], Anita P. Pax[a,b], Adabelle Ong[a,b], Jitraporn Vongsvivut[c], Mark J. Tobin[c], Sandra E. Kentish[b], Sally L. Gras[a,b,*]

[a]The Bio21 Molecular Science and Biotechnology Institute, The University of Melbourne, Parkville, Victoria 3010, Australia.

[b]The ARC Dairy Innovation Hub, The Department of Chemical and Biomolecular Engineering, The University of Melbourne, Parkville, Victoria 3010, Australia.

[c]Infrared Microspectroscopy (IRM) Beamline, ANSTO - Australian Synchrotron, 800 Blackburn Road, Clayton, Victoria 3168, Australia.

*Corresponding author: sgras@unimelb.edu.au (S.L. Gras)

Tel.: +61-3-8344 6281; fax: +61-3-8344 4153

15 Highlights

16 - Variation in acid gel pH affects the microstructure of cream cheese
17 - Greater protein hydration at pH 5.0 leads to bigger protein-fat aggregates
18 - Reduced interaction between whey protein and casein contributes to softer cheese
19 - Aggregated β-sheet protein increases and β-turn protein decreases in cheese at pH 4.3

Abstract

The effect of variation in acid gel pH during cream cheese production was investigated. The gel microstructure was denser and cheese texture firmer, as the pH decreased from pH 5.0 to pH 4.3, despite the viscoelasticity of these gels remaining similar during heating. Protein hydration and secondary structure appeared to be key factors affecting both cheese microstructure and properties. Proteins within the matrix appeared to swell at pH 5.0, leading to a larger corpuscular structure; greater β-turn structure was also observed by synchrotron-Fourier transform infrared (S-FTIR) microspectroscopy and the cheese was softer. A decrease in pH led to a denser microstructure with increased aggregated β-sheet structure and a firmer cheese. The higher whey protein loss at low pH likely contributed to increased cheese hardness. In summary, controlling the pH of acid gel is important, as this parameter affects proteins in the cheese, their secondary structure and the resulting cream cheese.

Keywords: Cream cheese; Microstructure; Fat and protein aggregates; pH of cheese; Rheological properties, Texture, Synchrotron FTIR microspectroscopy, Protein secondary structure

1. Introduction

A number of factors affect the properties of cream cheese including: the milk composition and processing parameters (Brighenti, Govindasamy-Lucey, Jaeggi, Johnson, & Lucey, 2018), the pH of the cheese (Aliste & Kindstedt, 2005; Monteiro, Tavares, Kindstedt, & Gigante, 2009), the degree of whey separation and moisture content of the cheese (Ong, Kentish, & Gras, 2018), the homogenization of curd (Sanchez, Beauregard, Chassagne, Bimbenet, & Hardy, 1994) and the cooling rate of the cheese (Sanchez, Beauregard, Chassagne, Duquenoy, & Hardy, 1994). The cheese microstructure also influences product texture and functionality (Everett & Auty, 2008). Previous studies, however, have mainly focused on the rheological properties of cream cheese, with only a few reports describing the impact of the microstructure of cream cheese on product functionality.

pH is a particularly important parameter during cream cheese production. The pH of cream cheese may vary, especially in a semi-continuous process where a large tank is used for fermentation. The final pH after fermentation is normally controlled by cooling a single batch in a fermentation tank or by mixing batches with different pH. This is followed by heat treatment for whey separation, which effectively stops the activity of the starter culture, preventing further changes in pH. The pH at the point of whey separation is known to affect product texture, as a pH > 4.7 was reported to produce cream cheese with soft texture and a pH < 4.6 resulted in cheese with a grainy texture (Lucey, 2011). The underlying factors that led to these changes in texture, however, have not been described. Other studies have examined the effect of pH from 4.0 to 7.2 by exposing the finished cheese to an atmosphere of a volatile base such as ammonia, or a volatile acid such as acetic acid (Aliste et al., 2005; Monteiro et al., 2009). The protein network that surrounded the fat droplets within the cheese matrix was reported to increase in volume with increasing pH, possibly due to the swelling of the casein network. Whilst the use of a volatile acid or base solution provides some scientific insights, it is not consistent with industry practice, suggesting that further detailed study of the changes that occur *in situ* during production will improve our understanding of the impact of this processing variable on product functionality.

Changes in pH affect the charge of a protein, the protein conformation and its stability against denaturation. Previous studies have investigated the effect of pH on whey protein denaturation in several media including whey (Donovan & Mulvihill, 1987), distilled water with purified proteins (de Wit & Klarenbeek, 1984) and milk (Anema, 2018). The stability of α-lactalbumin (LA) in whey was reported to be relatively independent of pH, while β-lactoglobulin (LG) was found to be less stable at higher pH such as pH 6.7 (Donovan et al., 1987). Similarly, in pH adjusted water, the thermostability of β-LG decreased as the pH increased from pH 3.0 to pH 7.5 (de Wit et al., 1984). In milk, the level of denaturation of β-

LG and α-LA was also reported to increase as the pH became more alkaline from pH 5.2 to pH 8.8 (Law, Banks, Horne, Leaver, & West, 1994).

The association of whey and casein proteins is also determined by the pH at which the sample is heated (Vasbinder & de Kruif, 2003). Heat treatment results in the exposure of the reactive thiol in β-LG that can form disulphide bonds with other proteins including κ-casein, α_{s2}-casein and α-LA. The α-LA lacks free thiol groups but has four disulphide bridges that can bind to the thiol groups of β-LG. Oldfield et al. (2000) showed that the association of both β-LG and α-LA with the casein micelles increased at pH 6.48 compared to pH 6.83, but this study did not extend to the pH range relevant to the heating of acid milk gels during cream cheese production (i.e. pH 4.3 – pH 5.0). The changes in pH or temperature also affects protein secondary structure and has been shown to impact on the functionality of individual isolated proteins (Georget & Belton, 2006; Pikal-Cleland, Rodriguez-Hornedo, Amidon, & Carpenter, 2000).

Changes in pH also affect the solubility of calcium and the total calcium in cheese. In milk, the calcium in the colloidal phase solubilizes during acidification and becomes completely soluble in the aqueous phase at pH 3.5 (Wolfschoon-Pombo & Andlinger, 2013). The total calcium remaining in cream cheese therefore depends on the pH at which the curd is separated from the whey. The total calcium in natural cheeses, such as Cheddar, ranges from 20-40 mg/g protein, whereas in acid curd cheeses the remaining calcium is only <6 mg/g of protein for Cottage cheese and 10 mg/g protein for cream cheese, due to the low pH of the curd after the whey removal (Wolfschoon-Pombo et al., 2013).

Understanding how pH affects the aggregation of protein and fat during cream cheese making and how whey protein and calcium contributes to this structure is important, as this information will allow a more complete understanding of how the unique structure of cream cheese is developed. This information can also be used by manufacturers to optimise and tailor the final microstructure and texture of the cheese. The current study aims to understand how variation in the pH of acid gels typical of cream cheese manufacture, affects the microstructure of the gel and the whey properties and how these changes subsequenty affect the microstructure and texture of the final product. We also apply a new synchrotron Fourier transform infrared (S-FTIR) microspectroscopy method (Pax, Ong, Vongsvivut, Tobin, Kentish, & Gras, 2019) to examine how these changes in pH affect the conformation of proteins within the structure of cream cheese in its natural condition with minimal sample preparation.

2. Material and Methods

2.1. Production of cream cheese with different pH

Milk standardized to a final concentration of 12.0 ± 0.4 % (w/w) fat and 3.3 ± 0.1 % (w/w) protein, homogenized at 14 MPa at 55 °C and pasteurized at 72 °C for 15 s was collected from a commercial plant (Victoria, Australia). The processed milk was stored in a 4 °C cold room and used for cream cheese-making within 1 week.

Eight batches of cream cheese were prepared (two independent batches for each of four pH treatments). For each batch, 2 kg of of milk was tempered to 22 °C in a kettle (GSM Sales, Rose Park, Australia) with stirring at 500 revolutions per minute (rpm) for 30 min prior to the addition of 0.01 % w/w frozen mesophilic starter culture (Chr. Hansen, Victoria, Australia). The final pH (4.3, 4.5, 4.7 or 5.0) was controlled by adjusting the time of the fermentation, which ranged between 14-19 h. When the target pH was achieved, the fermentation was stopped by heating the acidified milk gel to 80 °C for 10 min with stirring at 500 rpm. This was followed by centrifugation in a Sorvall RC6 Plus centrifuge (Thermo Scientific, Victoria, Australia) at 5,000 x g for 10 min according to a previously published protocol (Ong et al., 2018) to separate the curd from the whey.

To standardize the moisture content in the final cheese, a small portion of the expelled whey was added back to the kettle with the curd. The following equations were used to achieve a standard moisture content of 52 % w/w in the final cheese or total solids of 48 % w/w (*Ts cheese*). First, a theoretical target weight of whey was estimated based on the initial total solids of the milk (*Ts milk*, 20.8 ± 0.2 % w/w) and total solid of the whey (*Ts whey*, 6.6 ± 0.1 % w/w):

$$Target\ whey\ separation = Weight\ of\ milk - \left(\frac{Ts\ milk - Ts\ whey}{Ts\ cheese - Ts\ whey}\ x\ Weight\ of\ milk\right) \quad (1)$$

The amount of whey to be added to the curd was then calculated from the difference between the actual weight of whey separated during cheese making and the theoretical target whey separation:

$$Whey\ added = Actual\ whey\ separated - Target\ whey\ separation \quad (2)$$

After centrifugation, the curd samples were immediately re-heated in a kettle to 80 °C with stirring at 500 rpm for 10 min followed by the addition of a mixture of sodium chloride at 1 % w/w of curd, locust bean gum at 0.25 % w/w of curd and guar gum at 0.25 % w/w of curd. The heat treatment continued for another 30 min at 80 °C and the hot cheese was packed in 200 mL sample containers prior to storage at 4 °C.

145 ***2.2. Microstructure analysis***

146 The microstructure of the gel and cream cheese samples were analysed using an
147 inverted Leica SP8 confocal laser scanning microscopy (CLSM, Leica Microsystems,
148 Heidelberg, Germany). Samples were stained with Nile Red and Fast Green FCF (both from
149 Sigma, Victoria, Australia), as described previously (Ong et al., 2018). Cheese samples were
150 also analysed using a field emission gun scanning electron microscope (SEM, Quanta, FEI,
151 Oregon, USA) following an established method (Ong, Dagastine, Kentish, & Gras, 2011).
152 Two samples were prepared for each batch of cheese giving a total of four samples
153 analysed for each pH treatment and representative images are presented.

154 Image analysis of the CLSM images was performed using Imaris software (Bitplane,
155 South Windsor, CT, USA), as previously described (Ong et al., 2011). In brief, a 3D image
156 was constructed from 20-30 layers of 2D images with the separation between plane set to
157 0.3 μm, giving a total image depth of 6-9 μm. The porosity was assessed by examining the
158 fraction of the non-stained section of the 3D image of the gel.To quantify the size of the
159 corpuscular structure, a new surface was created only for the fat channel using the 'create
160 surface' function and the particle size quantified in Imaris. The close proximity of multiple fat-
161 protein clusters prevented thresholding of individual clusters with both protein and fat
162 present. By applying thresholding to the fat aggregates, clearly separated clusters could be
163 obtained and could be used as an indicator for changes within the corpuscular structure.
164 Within the cheese microstructure, there are also free fat particles and large corpuscular
165 structures > 10 μm in size. These large structures were also quantified by calculating the
166 percentage of fat particles where the largest diameter was > 10 μm.

167

168 ***2.3. Texture analysis***

169 The firmness of the gel and cream cheese samples were measured at 10 °C ± 1 °C
170 using a TA.HD texture analyser (Stable Micro Systems, Surrey, UK) equipped with a 5 kg
171 load cell. Samples were tempered to 10 °C in an incubator (Thermoline, Victoria, Australia)
172 prior to analysis. Cylindrical probes 10 mm in diameter or 5 mm in diameter were used for
173 the gel and cheese samples respectively during the penetration test. The trigger force was
174 set to 3 g and the test speed was set to 2 mm/s and 5 mm/s for the gel and cream cheese
175 samples respectively. The firmness of the samples was recorded as the maximum force
176 required to penetrate the samples by 10 mm. The texture measurement was performed in
177 triplicate for each batch, giving a total of six samples analysed for each pH treatment. The
178 data are presented as the mean ± the standard deviation of the mean (n = 6).

179

180 ***2.4. Rheological properties***

181 The rheological properties of the gels were assessed using an AR-G2 rheometer (TA
182 Instrument, New Castle, USA). Temperature sweep analysis from 20 °C to 90 °C was
183 performed using a parallel plate 40 mm in diameter and the temperature increment was set
184 at 5 °C for 90 s. A strain of 0.1 % was used as it was found to be within the linear
185 viscoelastic region (LVR). Two gel samples were analysed for each batch (i.e. 4 samples for
186 each pH treatment) and the data are presented as the mean ± the standard deviation of the
187 mean (n = 4).
188 Cream cheese samples were prepared for rheological analysis following a published
189 method (Ong et al., 2018). Briefly, the cheese samples were formed into a cylindrical shape
190 of 10 mm in height and 20 mm in diameter using a plastic syringe with the end of the syringe
191 removed. The sample was analysed at 10 °C, as this temperature is most commonly used
192 for further processing of cream cheese (e.g. for baking). A frequency sweep from 1 Hz to
193 100 Hz at a constant strain of 0.01 % was performed for the cheese samples using a 40 mm
194 parallel plate with the gap set to 2 mm. Two analyses were conducted for each batch of
195 cheese in each trial. A total of 4 measurements were obtained for each pH treatment and the
196 data presented are the mean ± the standard deviation of the mean (n = 4).
197
198 ***2.5. Protein profiles of whey at different pH***
199 Sodium dodecyl sulphate polyacrylamide gel electrophoresis (SDS-PAGE) was used to
200 analyse the protein within the whey samples collected for cheese processed at different pH.
201 Samples 8 µL in volume were prepared and loaded onto a 4-12 % tris-glycine gel (Life
202 Technologies, Victoria, Australia). The gel was scanned using a Fuji Film Dark Box
203 (Brookvale, Australia) and the intensity of the band was analysed using Fuji Film LAS 3000
204 software.
205 A molecular weight ladder (Precision Plus, Bio-Rad, Victoria, Australia) and a whey
206 sample obtained during cream cheese production where heat was not applied prior to whey
207 separation (Ong et al., 2018) were also loaded in duplicate, together with the experimental
208 whey samples. This reference sample allows a semi-quantitative comparison of the degree
209 of denaturation of the different whey proteins including β-lactoglobullin or α-lactalbumin
210 relative to the whey proteins present in the unheated sample (Ong et al., 2018). The results
211 were plotted as the mean ± the standard deviation of the mean (n = 4).
212
213 ***2.6. Composition of whey and cream cheese***
214 The protein content of the whey and cream cheese samples was analysed using an
215 elemental analyser (LECO Corporation, Saint Joseph, MI, USA) where the nitrogen
216 concentration was multiplied by a factor of 6.38. The fat content was analysed using the
217 Babcock Method . The moisture content and dry matter were analysed by drying samples in

218 an oven overnight at 102 °C. The pH of the samples was measured using a Mettler Toledo
219 pH meter that was calibrated against pH 4.0 and pH 7.0 calibration solutions (Port
220 Melbourne, Victoria, Australia). The protein, fat and moisture analysis were performed in
221 duplicate for each batch of cheese and the results are presented as the mean ± the standard
222 deviation of the mean (n = 4).
223 The calcium content of the whey and cream cheese samples was analysed using
224 inductively coupled plasma optical emission spectrometry (ICP-OES, Varian Inc., PaloAlto,
225 CA, USA). Whey samples were diluted 100 times in purified water with a resistivity of 18.2
226 MΩ cm (Millipore MilliQ, Billerica, MA, USA). The cream cheese samples (1 g) were dried at
227 102 °C overnight prior to ashing at 600 °C for 6 h in a chamber furnace (Shimaden, Tokyo,
228 Japan). The ashes were dissolved in 1 mL of nitric acid (68 %) and 1 mL of hydrochloric acid
229 (32 %) (both from Univar, Ingleburn, NSW, Australia) followed by dilution with purified water
230 to a total volume of 10 mL. A series of calcium chloride dihydrate (Merck, Bayswater, Vic,
231 Australia) standard solutions (0-1.36 mg/mL) were also analysed and used as a standard
232 curve to estimate the concentration of calcium in the whey or cheese samples. The data are
233 plotted as the mean ± the standard deviation of the mean (n = 2).
234
235 ***2.7. Synchrotron Fourier transform infrared microspectroscopic analysis of cream***
236 ***cheese***
237 The S-FTIR data collection, processing and analysis were performed following our
238 previously published method (Pax et al., 2019). In brief, the measurement was conducted at
239 the Australian Synchrotron Infrared Microspectroscopy (IRM) Beamline (Victoria, Australia),
240 using an in-house adapted macro-attenuated total reflection (macro-ATR) device
241 (Vongsvivut et al., 2019) coupled with a 250 µm diameter facet germanium (Ge) ATR crystal
242 and a water circulating temperature control unit (Huber Ministat®, Scitek, New South Wales,
243 Australia). The IRM beamline was equipped with a Bruker Vertex 80v spectrometer coupled
244 with a Hyperion 2000 FTIR microscope and a liquid nitrogen-cooled narrow-band mercury
245 cadmium telluride (MCT) detector (Bruker Optik GmbH, Ettlingen, Germany). All S-FTIR
246 spectra were recorded within a spectral range of 3800-700 cm^{-1} using 4 cm^{-1} spectral
247 resolution operated by OPUS 7.2 software suite (Bruker).
248 Chemical maps (60 µm x 60 µm) of cream cheese samples produced at pH 4.3, 4.5 and
249 5.0 were acquired with a focused beam 3.1 µm in diameter with a step interval of 1 µm. Two
250 cream cheese samples were analysed for each pH treatment and representative chemical
251 images and average spectra are presented. This analysis resulted in the acquisition of 3600
252 spectra for each replicate sample.
253 Atmospheric compensation was first performed using the OPUS 7.2 software (Bruker), to
254 remove interference from atmospheric water and carbon dioxide from the spectra. Next the

resultant absorbance spectra in each chemical map were pre-processed using a noise reduction algorithm, second derivatization with 13 smoothing points and vector normalization in CytoSpec™ v. 1.4.02 software (Cytospec Inc., Boston, MA, USA).

Hierarchical cluster analysis (HCA) was subsequently performed using the pre-processed and normalized second derivative spectra using two spectral ranges that contain the biological bands of interest corresponding to lipids and proteins (i.e. 3000-2800 cm^{-1} and 1800-1100 cm^{-1}). The HCA discriminated the spectra in each chemical map into five clusters according to their spectral features. In this study, only the clusters that contained spectra with high protein to fat ratio were selected (approximately 350-750 spectra for each replicate group) and subsequently processed for the principal component analysis (PCA) using The Unscrambler® 10.1 software package (CAMO Software AS, Oslo, Norway), as previously described by Pax et al. (2019).

Prior to PCA, the spectra were also processed using an extended multiplicative scatter correction (EMSC) algorithm, based on the same spectral regions that contain biological bands associated with proteins and lipids (i.e. 3000-2800 cm^{-1} and 1800-1100 cm^{-1}). In principle, the EMSC algorithm removes light scattering artefacts and normalizes the spectra accounting for pathlength differences, which reportedly yields more robust calibration models and thereby an improved discrimination accuracy. After that, PCA was conducted on the same biological regions (3000-2800 cm^{-1} and 1800-1100 cm^{-1}), as well as on the amide I protein region alone (1700-1600 cm^{-1}).

2.8. Data analysis

Statistical analysis was carried out using the Minitab statistical package (Minitab Inc, State College, PA, USA), where one way analysis of variance and Tukey's paired comparison were used to compare the statistical significant between means. A significance level $\alpha = 0.05$ was used throughout the study.

3. Results and Discussions

3.1. The effect of pH on the gel properties

The microstructure of the acidified homogenized milk prepared for cream cheese making at different pH (pH 4.3, 4.5, 4.7 and 5.0) was first assessed. Such microstructure has been reported previously at pH 4.5, where 'fat clusters' or 'homogenization clusters', ~0.9 µm in diameter could be observed. These clusters form as a result of the high fat to protein ratio in the milk, which led to insufficient milk protein to cover the increased surface area of fat globules following homogenization (Ong et al., 2018).

The time taken to ferment these samples to the desired pH varied from ~14 to ~19 h (pH 4.3, 19 ± 2 h; pH 4.5, 17 ± 1 h; pH 4.7, 15 ± 0 h and pH 5.0, 14 ± 2 h). As the pH reduced

292 during fermentation, the protein and fat clusters aggregated further forming a three
293 dimensional network (Fig. 1a). Pores containing the aqueous serum could be observed but
294 the fat clusters were less visible in this gelled structure. The protein and fat network was
295 found to be more continuous at a lower pH (e.g. pH 4.3), with smaller pores compared to the
296 more porous microstructure observed at a higher pH (e.g. pH 5.0). The porosity of the gel
297 determined by image analysis clearly decreased as the pH decreased to pH 4.3, confirming
298 this visual observation (Fig. 1b).

299 The physico-chemical mechanisms involved in the formation of the gel network during
300 acidification of homogenized milk has been reported in previous studies (Lucey, Munro, &
301 Singh, 1998). At pH ~5.0 or lower, colloidal calcium phosphate (CCP) is fully solubilized in
302 milk but a small proportion of CCP may remain in cheese, possibly due to the protective
303 effect of the greater solids concentration (Lucey & Fox, 1993). As the pH becomes close to
304 the isoelectric point of casein (pH 4.6), the net negative charge on the casein decreases,
305 which leads to a decrease in electrostatic repulsion, an increase in hydrophobic interactions
306 between casein molecules and an increase in aggregation. In this study, aggregation was
307 observed at all final pH. At pH 5.0, however, the gel was much softer than at a lower pH (Fig.
308 1b). At high pH above the isoelectric point of casein (i.e. pH 4.6), aggregation is known to
309 occur in heat treated milk samples due to the denaturation of β-LG, which has a higher
310 isoelectric point (~pH 5.3) (Lucey et al., 1998). The gel firmness continues to increase as the
311 pH of the sample decreases closer to the isoelectric pH of casein, due to the increased
312 aggregation including casein aggregation, consistent with the decreased porosity observed
313 for these samples.

314 In cream cheese making, the acidified gel is usually heated once the targeted pH is
315 achieved, stopping the activity of the starter culture and facilitating whey separation. The
316 properties of the gels during heating from 20 °C to 90 °C were therefore assessed in a series
317 of temperature sweep experiments using a rheometer, as shown in Fig. 1c. In general, the
318 differences in gel pH did not change the temperature sweep profile or the trend in storage
319 modulus (G'), loss modulus (G") and delta tangent (δ). The G' was higher than the G" for all
320 samples, an observation typical of elastic gel structures. The starting G' was higher for
321 samples with a lower pH, consistent with the greater gel firmness observed for these
322 samples but no significant differences could be observed between the pH treatments as the
323 temperature increased.

324 In all samples, the structure appeared to weaken during heating from 20 °C to 60 °C, as
325 indicated by a decrease in G', possibly due to the liquefaction of fat and the loss of structural
326 support due to fat coalescence. The similar trends indicate that the fat melting point is
327 independent of the sample pH, as may be expected. Around ~55 °C, the delta tangent was

328 the highest for all samples, suggesting the samples had a lower elasticity at this
329 temperature, again regardless of gel pH.
330 Increases in G' above 80 °C were not statistically significant. More prolonged heating,
331 however, may potentially lead to significant protein aggregation. For example, Modler et al.
332 (1989) observed a grittiness in cheese spread made from vat-pasteurized milk heated at 63
333 °C for 30 min followed by curd heat treatment at 80 °C for 10 min that was attributed to the
334 presence of particles consisting mainly of compacted protein. Further study is required to
335 examine the link between the heating rate of the acid gel and the potential development of
336 such grittiness.
337
338 ***3.2. The effect of pH on whey and cream cheese composition***
339 The changes in gel microstructure observed in Fig. 1a as a function of pH led to
340 changes in the water holding capacity and the amount of whey released during cheese-
341 making (Fig. 2a). The volume of whey released was significantly lower ($P < 0.05$) at the
342 lowest pH measured, possibly due to the higher gel strength (de Kruif, S.G., Zhu, Havea, &
343 Coker, 2015). To standardize the moisture content of the samples during cheese making, as
344 occurs in industry practice, a portion of whey was added back to the kettle, along with the
345 curd, as described in Section 2.1. In this way, the moisture content of the final cream cheese
346 was statistically similar ($P > 0.05$, Fig. 2b) minimizing the effect of moisture variation on the
347 properties of the cheese.
348 The amount of calcium lost in the whey was significantly higher ($P < 0.05$) at lower pH
349 (i.e. pH 4.3, pH 4.5 and pH 4.7) compared to at pH 5.0 (Fig. 2c). This was expected, as
350 calcium is more soluble at a lower pH (Wolfschoon-Pombo et al., 2013). The higher calcium
351 loss resulted in lower total calcium in the cream cheese with lower pH. Only a small amount
352 of fat or protein was lost in the whey and the concentration of fat and protein was not
353 significantly affected by the pH treatment ($P > 0.05$) (Fig. 2d). As a result, the fat and protein
354 composition of the final cream cheese did not significantly differ ($P > 0.05$) (Fig. 2e).
355 Changes to the protein profile in the whey is one consequence of changes in the pH of
356 the acid gel. The heat treatment of milk is known to cause several complexes including i) the
357 association of whey proteins with casein micelles mainly through β- LG and κ-casein ii) the
358 interaction of α–LA with β-LG and iii) the interaction of whey proteins with fat globules
359 (Corredig & Dalgleish, 1996, 1999). In this study, the gels acidified to different pH were
360 heated to 80 °C for 10 min prior to whey separation and the protein profiles of the samples
361 within the whey at different pH were then examined using SDS-PAGE (Fig. 2f,
362 Supplementary Information Fig. 1).
363 As expected, the extent of denaturation of α-LA in the samples was greater than β-LG
364 due to the higher denaturation temperature of β-LG (65.2 °C vs 72.8 °C for α-LA and β-LG,

365 (Ruegg & Moor, 1977). The intensity of the band of β-LG and α-LA in the heat treated whey
366 samples relative to the intensity of the band in the sample without heat treatment was within
367 75-95 % compared to 30-65 % for α-LA and β-LG, respectively (Fig. 2f). Lactoferrin (LF) and
368 serum albumin (SA) that were present in the unheated samples, were not detected in any of
369 the heat treated whey samples, regardless of pH (Supplementary Information Fig. 1). This
370 was expected due to the lower denaturation temperature of LF and SA (64.7 °C and 62.2 °C,
371 respectively at pH 6.7).

372 The pH treatment significantly affected the extent of α-LA denaturation ($P < 0.05$), with
373 less α-LA in the whey at lower pH, indicating a higher level of denaturation and better
374 retention in the cream cheese. The pH treatment did not significantly influence the β-LG
375 denaturation ($P > 0.05$). Fig. 2f shows ~25 % less α–LA was captured in the whey at pH 4.3
376 compared to at pH 5.0. Previously, lowering the pH has been shown to significantly
377 decrease the denaturation temperature of α-LA from 61.5 °C at pH 6.5 to 58.6 °C at pH 3.5
378 but no difference in the denaturation temperature was reported in pH range of 6.5-4.5. The
379 effect of lower pH observed in this study was possibly due to the lower denaturation
380 temperature of α–LA at pH below 4.5 (Bernal & Jelen, 1984). No significant variation in the
381 heat denaturation of β-LG has been reported in the pH range of 6.3-7.3 (Ruegg et al., 1977)
382 and conversley a separate study reported an increase in denaturation temperature from 71
383 °C at pH 8.6 to 85 °C at pH 3, making β-LG more resistant to denaturation at lower pH
384 (Boye, Ma, Ismail, Harwalkar, & Kalab, 1997). This possibly explains the low extent of
385 denaturation of β-LG when the sample was heated to 80 °C at the pH range within 5.0-4.3
386 examined in this study.
387

388 ***3.3. The effect of pH on cream cheese microstructure***

389 The microstructure of cream cheese observed using CLSM (Fig. 3a) and cryo SEM (Fig.
390 3b) were also affected by the pH treatment examined here. This microstructure consists of a
391 corpuscular structure, characterized by clusters of small fat globules coated extensively with
392 protein aggregates, as shown by the white circles. Cream cheese produced from acid gels
393 with a lower pH had a more aggregated structure. Decreased electrostatic repulsion and
394 increased hydrophobic interaction at low pH possibly contributed to the observed increase in
395 aggregation, as the proteins were closer to the iso-electric point of caseins at pH 4.6, as the
396 pH decresed.

397 The size of the corpuscular structure also appeared to decrease as the cheese pH was
398 reduced from pH 5.0 to pH 4.7 (Fig. 3a and 3b). This observation was confirmed in
399 quantitative analysis of 3D images using an imaging software. The fat within these images
400 was rendered separately, as illustrated in the representative 3D images of the cream cheese
401 at pH 5.0 (Fig. 3c), as the close proximity of multiple fat-protein clusters prevented

402 thresholding of individual clusters with both protein and fat present. Using this method,
403 clearly separated fat clusters could be obtained and used to demonstrate the change in the
404 size of the corpuscular structure. The average size of the clusters decreased significantly (P
405 < 0.05) from ~5 μm in size for cream cheese at pH 5.0 to ~4 μm in size for cream cheese at
406 pH 4.7 to pH 4.3 (Fig. 3d). Fig. 3e shows that the proportion of the fat clusters with a size
407 greater than 10 μm was similar for cream cheese at pH 4.3 – pH 4.7, but was significantly
408 higher ($P < 0.05$) in cream cheese at pH 5.0 when compared to cream cheese at pH 4.3 or
409 pH 4.7.

410 The protein networks within cheese are known to swell for a number of reasons. A
411 previous study indicated that this was potentially due to the increased hydration and
412 interaction between protein and water (Monteiro et al., 2009). In Mozzarella cheese, a lower
413 level of casein-associated calcium at lower pH is also known to promote casein-water
414 interactions that lead to protein swelling (McMahon, Fife, & Oberg, 1999). In this study,
415 protein swelling was visible in the cream cheese made from gels at a higher pH. While
416 greater calcium loss was observed in the whey at pH 4.3 – pH 4.7 (Fig. 2c), the smaller
417 quantity of casein-associated calcium is less likely to play a role in cream cheese compared
418 to its role in medium or hard cheeses. This is because the total calcium content (Fig. 2c) is
419 10 times lower than the total calcium level in Mozzarella cheese.

420 The capacity for water absorption in acid-precipitated casein was reported to be at its
421 lowest in the pH ranges of 4.6 – pH 4.0 and increased as the pH increased towards neutral
422 pH (Ruegg & Blanc, 1976). This increased water absorption capacity at pH 5.0 compared to
423 pH 4.3 – pH 4.7 possibly contributed to the bigger corpuscular structure observed in this
424 study. At low pH, increased hydrophobic protein-protein interactions may cause the protein
425 structure to contract, resulting in a smaller corpuscular structure, an observation that is
426 consistent with a previous study (Monteiro et al., 2009). Minimum swelling at pH near the
427 isoelectric point of a whey protein hydrogel has also been previously reported
428 (Gunasekaran, Ko, & Xiao, 2007). Changes in the secondary structure could also contribute
429 to the changes in the corpuscular structure (see Section 3.5).

430 A schematic diagram summarizing the development of the microstructure of cream
431 cheese at different pH is presented in Fig. 4. During fermentation, the clusters of fat and
432 protein in the homogenised milk (Fig. 4a) aggregate as a result of charge neutralization, this
433 occurs to a greater extent at lower pH. The increase in aggregation and network formation
434 leads to a gel structure with smaller pores as compared to the larger pores observed at
435 higher pH (Fig. 4c, Fig. 1a). These smaller pores trap more whey, resulting in less whey
436 expulsion (Fig. 2a). At lower pH, greater CCP solubilisation leads to a higher calcium
437 concentration in the whey (Fig. 2c). The heat treatment of the gel causes shrinkage, whey
438 expulsion and the denaturation of whey protein (Fig. 4d, Fig. 2f). The denatured whey

439 protein is retained with the curd during whey separation. Heat treatment of the curd at 80 °C
440 and shearing at 500 rpm helps to disperse the gum, which binds the free serum within the
441 structure, preventing syneresis (Macdougall, Ong, Palmer, & Gras, 2019). The greater water
442 absorption capacity of the protein at higher pH leads to an increase in the size of the
443 corpuscular structure within the cheese (Fig. 3e).
444 Within the cheese microstructure there are also regions of coalesced fat (Fig. 4e), as
445 shown by the white arrows in Fig. 3a. The appearance of the coalesced fat within the
446 cheese, however, is not homogenous and could not be quantified within this study.
447
448 ***3.4. The effect of pH on texture and rheological property of cream cheese***
449 The firmness of the cream cheese increased when the pH was reduced from pH 5.0 to
450 pH 4.7 (Fig. 3f) but was not significantly different ($P > 0.05$) from pH 4.7 – pH 4.3. The
451 swelling of the protein, which led to larger corpuscular structures (Fig. 3a and 3b), possibly
452 contributed to the softer cheese at pH 5.0. These larger corpuscular structures could also
453 reduce particle to particle interactions, which may affect the firmness of the cheese. Further,
454 at this pH there are fewer interactions of whey proteins with caseins, as indicated by the
455 greater whey protein loss to the whey (Fig. 2f), which may also contribute to the lower
456 hardness of the cheese. This has been reported previously for acid gels, where milk without
457 added whey protein had a lower gel stiffness compared to samples where whey protein was
458 added, when heated to 80 °C for 30 min (Anema, 2018). Our observation is also consistent
459 with previous studies (Monteiro et al., 2009), where the firmness of cream cheese was
460 reported to be lower at higher pH.
461 A frequency sweep during rheological analysis shows a significant increase in the
462 storage modulus of the cream cheese at pH 4.7 – pH 4.3 compared to at pH 5.0
463 (Supplementary Information Fig. 2), consistent with texture analysis. These results illustrate
464 the importance of controlling the pH of the cheese for optimum product texture and
465 consistency. Whilst our study sought to change the pH uniformly across the sample, it also
466 illustrates the potential of gradients of pH and heterogeneity within the acid gel that lead to
467 changes within the product.
468
469 ***3.5. Synchrotron-FTIR microspectroscopic analysis of cream cheese***
470 S-FTIR microspectroscopy gave further evidence that the protein structure within the
471 cream cheese was altered as a function of acid gel pH. The synchrotron macro ATR-FTIR
472 technique used in this study, couples a highly intense synchrotron-IR beam into a high
473 refractive index Ge hemispherical crystal (n = 4.0) in the ATR mode (Vongsvivut et al.,
474 2019). This specific optical configuration leads to an improvement in spatial resolution to 1-3
475 μm comparable to CLSM and allows sub-micron step resolution between measurement

points suitable for high-resolution chemical mapping, whilst still maintaining a good spectral signal-to-noise ratio (i.e. high-quality spectra). In particular, the macro ATR-FTIR device can also be coupled with a water circulating temperature control unit, allowing the measurement of dairy products to be performed at 4 ºC, similar to their storage conditions, to ensure the accuracy of the chemical information obtained (Pax et al., 2019).

Only cheese samples with pH treatments of 4.3, 4.5 and 5.0 were included in the S-FTIR analysis, given that samples at pH 4.5 and 4.7 had similar properties for a number of other measures (Figs. 2 and 3). Figures 5a and 5b present the average high protein spectra of the cream cheese produced at pH 4.3, pH 4.5 and pH 5, in forms of absorbance and second derivative spectral formats, respectively. Second derivatization, in particular, has been widely used in spectroscopic analysis because the method not only eliminates baseline effect, but also allows detection and positive identification of band components that are hidden in the presence of a broad overlapping component, improving the accuracy of the analysis in both qualitative and quantitative perspectives.

In all cases, the S-FTIR spectra revealed common characteristic features attributable to the main components in the cream cheese including water, proteins and lipids. In the high wavenumber region, the broad band observed in the range of 3600-3100 cm^{-1} represents ν(O–H) stretching modes of water molecules in the samples, whilst the triplet bands found within 3000-2800 cm^{-1} spectral range are associated with ν(C–H) stretching vibrations of methyl ($–CH_3$) and methylene ($–CH_2$) groups from both proteins and lipids. In the low wavenumber region, the sharp peak at ~1745 cm^{-1} is assignable to ν(C=O) stretches of ester functional groups from lipids and fatty acids, and is therefore indicative of total lipids (Vongsvivut, Heraud, Zhang, Kralovec, McNaughton, & Barrow, 2012). In particular, the prominent bands at ~1650 and 1550 cm^{-1} are attributed to amide I and II modes of proteins, and are commonly known as the characteristic features of proteins (Barth, 2007). The amide I band, which primarily represents ν(C=O) stretches of the amide groups, is most often used for characterising secondary protein structures because changes in the band shape and its position reflect the contribution of different protein conformations in the analysed samples (Yang, Yang, Kong, Dong, & Yu, 2015). Therfore, the amide I band was the main peak used in this study for determining differences in protein conformation present in the cream cheese samples at different pH values. According to the second derivative features of the amide I band in Fig. 5b2, the spectra of the cream cheese produced at all three pH values (i.e. pH 4.3, 4.5 and 5.0) revealed the most intense amide I band within the range of 1639-1634 cm^{-1}, indicating that the main protein conformation in the samples is in the form of β-sheet structures (Barth, 2007). The slight shift of the amide I band observed for the cream cheese at pH 5.0 (occurring at 1639 cm^{-1} compared to at 1634 cm^{-1} at pH 4.3) suggests a subtle, yet

noticeable, change of ν(C=O) interaction in the protein molecules with the surrounding medium at a higher pH. A weak band at ~1666 cm^{-1} suggests the co-existence of a smaller number of β-turn protein structures (Barth, 2007) within the cheese.

In addition, FTIR spectral maps of the amide I bands were produced to reveal the distribution of β-sheet (1634 cm^{-1}) and β-turn (1666 cm^{-1}) protein structures in the cream cheese samples (Fig. 5c). A significant increase in the relative intensity of the β-turn conformation was qualitatively observed at higher pH (i.e. pH 4.5 and 5.0), along with a corresponding decrease in β-sheet conformation.

Principal component analysis (PCA) revealed differences in the molecular structure of the cream cheese at pH 4.3, pH 4.5 and pH 5 based on the spectral regions corresponding to both proteins and lipids (i.e. 3000-2800 cm^{-1} and 1800-1100 cm^{-1}, Fig. 6a) and the spectral region corresponding to amide I protein alone (1700-1600 cm^{-1}, Fig. 6c). When including both protein and lipid compositions in the PCA, the cream cheese samples produced at the three pH appeared to separate into distinct clusters along the PC2 axis, which accounted for 22 % of the total variability (Fig. 6a**).** According to the corresponding PC2 loadings plot (Fig. 6b), the separation is primarily caused by the strong loading at 1175 cm^{-1} (i.e. ν_s(C–O–C) of esters from lipid triglycerides and fatty acids), the loadings at 2928 cm^{-1} and 2916 cm^{-1} (i.e. ν(C–H) stretches from methyl and methylene groups of lipids) and the weak loading at 1750 cm^{-1} (i.e. ν(C=O) of esters from lipid triglycerides and fatty acids). These data suggest that differences in lipid composition are responsible for the separation. In addition, a subtle change in the β-sheet protein structure was also observed, as a very weak loading at 1637 cm^{-1}, indicating a slightly higher amount of the β-sheet protein in the cream cheese at pH 4.3, consistent to the result presented in the chemical images in Fig. 5c.

When only the amide I region (1700-1600 cm^{-1}) was used in the PCA, the resultant scores plot in Fig. 6c clearly shows distinct separation of the spectral clusters from the three cream cheese groups along the PC1 axis, accounting for 61% of the variation. Based on the PC1 loadings plot (Fig. 6d), the separation was caused predominantly by the strong loading at ~1620 cm^{-1} attributed to aggregated intermolecular β-sheet structures (Lefevre & Subirade, 1999). This loading feature suggests that a greater amount of this form of aggregated β-sheet protein structure exists in the cream cheese produced at a lower pH (pH 4.3), compared to in the cream cheese produced at higher pH (pH 4.5 and pH 5), which is again consistent with the result previously obtained in FTIR spectral maps of the cheese (Fig. 5c). These aggregated structures are known to form as a result of heat treatment above 80 °C (Lefevre et al., 1999; Wu, Bertram, Kohler, Bocker, Ofstad, & Andersen, 2006). Also contributing to PC1 separation were peak shifts associated with β-sheet structures (1634-1639 cm^{-1}, Fig. 5b2), particularly at lower pH. These alterations are consistent with the

548 previously observed denaturation of whey proteins that led to an observed increase in
549 intermolecular anti-parallel β-sheet structures (Clark, Saunderson, & Suggett, 2009). The
550 PC1 separation is also associated with a higher proportion of β-turn structure (~1666 cm^{-1})
551 with higher pH (Fig. 5c). High concentrations of β-turn structure have been associated
552 increased protein hydration in wheat gluten (Georget et al., 2006). The increased protein
553 hydration at higher pH observed here is consistent with the increased size of the corpuscular
554 structure that was evident at higher pH, especially at pH 5 (Fig. 3).

555 In addition, the separation of the spectral clusters for cream cheese at pH 4.3 and pH 5
556 from clusters at pH 4.5 in the direction of the PC2 axes, as shown in the scores plot (Fig.
557 6c), can be explained using the PC2 loadings plot (Fig. 6d, at ~1670 cm^{-1}, 1653 cm^{-1} and
558 1634 cm^{-1}). These features suggest that proteins within the cream cheese formed at pH 4.3
559 and pH 5, likely differ in β-turn, α-helix and β-sheet structural conformation respectively,
560 compared to proteins within the cheese formed at pH 4.5.

561 The increase in aggregated β-sheet structure observed with decreasing cream cheese
562 pH is likely related to the denser microstructure and greater firmness observed in pH 4.3
563 samples. A more dense protein matrix has previously been observed with increased
564 aggregated β-sheet structure in other food samples, including foie gras (Théron et al., 2014),
565 providing further evidence that secondary structures are an important contributor to product
566 structure and function.

567

568 **4. Conclusions**

569 Good control of acid gel pH prior to whey separation is important to minimize variation in
570 cream cheese product microstructure and texture. Any variation in acid gel pH prior to whey
571 separation can alter the incorporation of whey proteins and calcium content of the cheese,
572 changing the resulting microstructure and texture. Protein swelling, larger corpuscular
573 structures, reduced interactions between whey proteins and casein and increased β-turn
574 protein structure all possibly contribute to the lower hardness of cream cheese at higher pH.
575 Conversley, a lower pH leads to a denser microstructure, smaller corpuscular structure,
576 increase in aggregated β-sheet protein structure and a firmer cream cheese product.
577 Knowledge of the contribution of pH to structure development in cream cheese improves our
578 understanding of the link between process parameters, microstructure and function and can
579 assist in the optimization and tailoring of product texture.

580

581 **Acknowledgements**

582 This project was supported by the funding provided by the Australian Research Council
583 Industrial Transformation Research Program (ITRP IH120100005). The ARC Dairy
584 Innovation Hub is a collaboration between The University of Melbourne, The University of

Queensland and Dairy Innovation Australia Ltd. Sally Gras and Lydia Ong are both supported by The ARC Dairy Innovation Hub. The authors would like to acknowledge the Advance Microscopy Facility (AMF), the Biological Optical Microscopy Platform (BOMP) at The Bio21 Institute of Molecular Science and Biotechnology Institute for access to equipment. S-FTIR data collection was undertaken at the IRM beamline at the Australian Synchrotron, part of ANSTO.

Conflict of interest

The authors declare no conflict of interest.

References

Aliste, M. A., & Kindstedt, P. (2005). Effect of increasing pH on texture of full and reduced-fat cream cheese. *Australian Journal of Dairy Technology, 60*(3), 225-230.

Anema, S. G. (2018). Effect of whey protein addition and pH on the acid gelation of heated skim milk. *International Dairy Journal, 79*, 5-14. https://doi.org/10.1016/j.idairyj.2017.11.008.

Barth, A. (2007). Infrared spectroscopy of proteins. *Biochimica Biophysica Acta, 1767*(9), 1073-1101. https://doi.org/10.1016/j.bbabio.2007.06.004.

Bernal, V., & Jelen, P. (1984). Effect of calcium binding on thermal denaturation of bovine α-lactalbumin. *Journal of Dairy Science, 67*(10), 2452-2454. https://doi.org/10.3168/jds.S0022-0302(84)81595-7.

Boye, J. I., Ma, C. Y., Ismail, A., Harwalkar, V. R., & Kalab, M. (1997). Molecular and microstructural studies of thermal denaturation and gelation of β-lactoglobulins A and B. *Journal of Agricultural and Food Chemistry, 45*(5), 1608-1618. https://doi.org/10.1021/jf960622x.

Brighenti, M., Govindasamy-Lucey, S., Jaeggi, J. J., Johnson, M. E., & Lucey, J. A. (2018). Effects of processing conditions on the texture and rheological properties of model acid gels and cream cheese. *Journal of Dairy Science, 101*(8), 6762-6775. https://doi.org/10.3168/jds.2018-14391.

Clark, A. H., Saunderson, D. H. P., & Suggett, A. (2009). Infrared and laser-raman spectroscopic studies of thermally-induced globular protein gels. *International Journal of Peptide and Protein Research, 17*(3), 353-364. https://doi.org/10.1111/j.1399-3011.1981.tb02002.x.

Corredig, M., & Dalgleish, D. G. (1996). Effect of different heat treatments on the strong binding interactions between whey proteins and milk fat globules in whole milk. *Journal of Dairy Research, 63*(3), 441-449. https://doi.org/10.1017/S0022029900031940.

Corredig, M., & Dalgleish, D. G. (1999). The mechanisms of the heat-induced interaction of whey proteins with casein micelles in milk. *International Dairy Journal, 9*(3-6), 233-236. https://doi.org/10.1016/S0958-6946(99)00066-7.

de Kruif, C. G., S.G., A., Zhu, C., Havea, P., & Coker, C. (2015). Water holding capacity and swelling of casein hydrogels. *Food Hydrocolloids, 44*, 372-379. https://doi.org/10.1016/j.foodhyd.2014.10.007.

de Wit, J. N., & Klarenbeek, G. (1984). E!ects of various heat treatments on structure and solubility of whey proteins. *Journal of Dairy Science, 67*, 2701-2710. https://doi.org/10.3168/jds.S0022-0302(84)81628-8.

Donovan, M., & Mulvihill, D. M. (1987). Thermal-denaturation and aggregation of whey proteins. *Irish Journal of Food Science and Technology, 11*(1), 87-100. <Go to ISI>://WOS:A1987L248300007.

Everett, D. W., & Auty, M. A. E. (2008). Cheese structure and current methods of analysis. *International Dairy Journal, 18*(7), 759-773. https://doi.org/10.1016/j.idairyj.2008.03.012.

Georget, D. M., & Belton, P. S. (2006). Effects of temperature and water content on the secondary structure of wheat gluten studied by FTIR spectroscopy. *Biomacromolecules, 7*(2), 469-475. https://doi.org/10.1021/bm050667j.

Gunasekaran, S., Ko, S., & Xiao, L. (2007). Use of whey proteins for encapsulation and controlled delivery applications. *Journal of food engineering, 83*(1), 31-40. https://doi.org/10.1016/j.jfoodeng.2006.11.001.

Law, A. J. R., Banks, J. M., Horne, D. S., Leaver, J., & West, I. G. (1994). Denaturation of the whey proteins in heated milk and their incorporation into Cheddar cheese. *Milchwissenschaft-Milk Science International, 49*(2), 63-67. <Go to ISI>://WOS:A1994NC07900001.

Lefevre, T., & Subirade, M. (1999). Structural and interaction properties of beta-Lactoglobulin as studied by FTIR spectroscopy. *International Journal of Food Science and Technology, 34*(5-6), 419-428. https://doi.org/10.1046/j.1365-2621.1999.00311.x.

Lucey, J. A. (2011). Cheese | Acid- and acid/heat coagulated cheese. In (pp. 698-705).

Lucey, J. A., & Fox, P. F. (1993). Importance of calcium and phosphate in cheese manufacture - a review. *Journal of Dairy Science, 76*(6), 1714-1724. https://doi.org/10.3168/jds.S0022-0302(93)77504-9.

Lucey, J. A., Munro, P. A., & Singh, H. (1998). Rheological properties and microstructure of acid milk gels as affected by fat content and heat treatment. *Journal of Food Science, 63*(4), 660-664. https://doi.org/10.1111/j.1365-2621.1998.tb15807.x.

Macdougall, P. E., Ong, L., Palmer, M. V., & Gras, S. L. (2019). The microstructure and textural properties of Australian cream cheese with differing composition. *International Dairy Journal, 9*, 104548. https://doi.org/10.1016/j.idairyj.2019.104548.

McMahon, D. J., Fife, R. L., & Oberg, C. J. (1999). Water partitioning in Mozzarella cheese and its relationship to cheese meltability. *Journal of Dairy Science, 82*(7), 1361-1369. https://doi.org/10.3168/jds.S0022-0302(99)75361-0.

Modler, H. W., Yiu, S. H., Bollinger, U. K., & Kalab, M. (1989). Grittiness in a pasteurized cheese spread - a microscopic study. *Food Microstructure, 8*(2), 201-210. <Go to ISI>://WOS:A1989CJ93800004.

Monteiro, R. R., Tavares, D. Q., Kindstedt, P. S., & Gigante, M. L. (2009). Effect of pH on microstructure and characteristics of cream cheese. *Journal of Food Science, 74*(2), C112-117. https://doi.org/10.1111/j.1750-3841.2008.01037.x.

Oldfield, D. J., Singh, H., Taylor, M. W., & Pearce, K. N. (2000). Heat-induced interactions of β-lactoglobulin and α-lactalbumin with the casein micelle in pH-adjusted skim milk. *International Dairy Journal, 10*, 509-518. https://doi.org/10.1016/S0958-6946(00)00087-X.

Ong, L., Dagastine, R. R., Kentish, S. E., & Gras, S. L. (2011). Microstructure of milk gel and cheese curd observed using cryo scanning electron microscopy and confocal microscopy. *Lwt-Food Science and Technology, 44*(5), 1291-1302. https://doi.org/10.1016/j.lwt.2010.12.026.

Ong, L., Kentish, S. E., & Gras, S. L. (2018). Small scale production of cream cheese: A comparison of batch centrifugation and cloth bag methods. *International Dairy Journal, 81*, 42-52. https://doi.org/10.1016/j.idairyj.2018.01.008.

Pax, A. P., Ong, L., Vongsvivut, J., Tobin, M. J., Kentish, S. E., & Gras, S. L. (2019). The characterisation of Mozzarella cheese microstructure using high resolution synchrotron transmission and ATR-FTIR microspectroscopy. *Food Chemistry, 291*, 214-222. https://doi.org/10.1016/j.foodchem.2019.04.016.

Pikal-Cleland, K. A., Rodriguez-Hornedo, N., Amidon, G. L., & Carpenter, J. F. (2000). Protein denaturation during freezing and thawing in phosphate buffer systems: monomeric and tetrameric beta-galactosidase. *Archives Biochemistry and Biophysics, 384*(2), 398-406. https://doi.org/10.1006/abbi.2000.2088.

Ruegg, M., & Blanc, B. (1976). Effect of pH on water-vapor sorption by caseins. *Journal of Dairy Science, 59*(6), 1019-1024. https://doi.org/10.3168/jds.S0022-0302(76)84318-4.

Ruegg, M., & Moor, U. (1977). Calorimetric study of the thermal denaturation of whey proteins in simulated milk ulrafiltrate. *Journal of Dairy Research, 44*, 509-520. https://doi.org/10.1017/S002202990002046X.

Sanchez, C., Beauregard, J. L., Chassagne, M. H., Bimbenet, J. J., & Hardy, J. (1994). Rheological and textural behaviour of double cream cheese. Part I: Effect of curd homogenization. *Journal of food engineering, 23*(4), 579-594. https://doi.org/10.1016/0260-8774(94)90113-9.

Sanchez, C., Beauregard, J. L., Chassagne, M. H., Duquenoy, A., & Hardy, J. (1994). Rheological and textural behaviour of double cream cheese. Part II: Effect of curd cooling rate. *Journal of food engineering, 23*(4), 595-608. https://doi.org/10.1016/0260-8774(94)90114-7.

Théron, L., Vénien, A., Jamme, F., Fernandez, X., Peyrin, F., Molette, C., . . . Astruc, T. (2014). Protein matrix involved in the lipid retention of foie gras during cooking: a multimodal hyperspectral imaging study. *Journal of Agricultural and Food Chemistry, 62*, 5954-5962. https://doi.org/10.1021/jf5009605.

Vasbinder, A. J., & de Kruif, C. G. (2003). Casein-whey protein interactions in heated milk: the influence of pH. *International Dairy Journal, 13*(8), 669-677. https://doi.org/10.1016/S0958-6946(03)00120-1.

Vongsvivut, J., Heraud, P., Zhang, W., Kralovec, J. A., McNaughton, D., & Barrow, C. J. (2012). Quantitative determination of fatty acid compositions in micro-encapsulated fish-oil supplements using Fourier transform infrared (FTIR) spectroscopy. *Food Chemistry, 135*(2), 603-609. https://doi.org/10.1016/j.foodchem.2012.05.012.

Vongsvivut, J., Perez-Guaita, D., Wood, B. R., Heraud, P., Khambatta, K., Hartnell, D., . . . Tobin, M. J. (2019). Synchrotron macro ATR-FTIR microspectroscopy for high-resolution chemical mapping of single cells. *Analyst, 144*(10), 3226-3238. https://doi.org/10.1039/c8an01543k.

Wolfschoon-Pombo, A. F., & Andlinger, D. J. (2013). Micellar calcium in acid curd cheese with different pH values, fat and protein levels. *International Dairy Journal, 32*(1), 20-25. https://doi.org/10.1016/j.idairyj.2013.03.011.

Wu, Z., Bertram, H. C., Kohler, A., Bocker, U., Ofstad, R., & Andersen, H. J. (2006). Influence of aging and salting on protein secondary structures and water distribution in uncooked and cooked pork. A combined FT-IR microspectroscopy and 1H NMR relaxometry study. *Journal of Agricultural and Food Chemistry, 54*(22), 8589-8597. https://doi.org/10.1021/jf061576w.

Yang, H. Y., Yang, S. N., Kong, J. L., Dong, A. C., & Yu, S. N. (2015). Obtaining information about protein secondary structures in aqueous solution using Fourier transform IR spectroscopy. *Nature Protocols, 10*(3), 382-396. https://doi.org/10.1038/nprot.2015.024.

716

717 **Figure legends**

718

719 Fig. 1. a) The microstructure of acid gel at pH 4.3, pH 4.5, pH 4.7 and pH 5.0 obtained using
720 CLSM. Nile red stained fat appears red and Fast green stained protein appears green. The
721 scale bar is 10 μm in length. b) The porosity of the gel determined by image analysis (□) and
722 the firmness of the gels measured using a texture analyser (●). c) The viscoelastic property
723 of the gels (●, storage modulus G'; □, loss modulus G" and ∆, delta tangent δ (G"/G')) during
724 temperature sweep analysis from 20 °C to 90 °C with the temperature increment set at 5 °C
725 for 90 s. Error bars are standard deviation of mean (n = 6 for gel firmness measurement and
726 n = 4 for temperature sweep analysis).

727

728 Fig. 2. a) The amount of whey released during cheese making. b) The moisture content of
729 the final cream cheese. (c) The concentration of total calcium in whey (◊) and in cheese (■).
730 (d) The concentration of protein (●) and fat (□) in whey. (e) The concentration of protein (●)
731 and fat (□) in cheese. (f) The proportion of undenatured whey protein (□, β–lactoglobullin
732 (LG) and ●, α–lactalbumin (LA)) relative to the concentration of β-LG and α-LA in the sample
733 without heat treatment. Errors bars are standard deviation of mean (n = 2 for whey released
734 and calcium concentration, n = 4 for moisture, fat, protein and whey analysis).

735

736 Fig. 3. Microstructures of cream cheese at pH 4.3, pH 4.5, pH 4.7 and pH 5.0, observed
737 using a) CLSM and b) cryo SEM techniques. Nile red stained fat appears red and Fast green
738 stained protein appears green in CLSM images. Circles indicate the corpuscular structure.
739 White arrows indicate fat coalesced. The scale bar is 10 μm in length. c) Representative 3D–
740 images of fat (red, left) and protein (green, right) constructed from 30 layers of 2D images
741 with gap between layers set at 0.3 μm giving a total thickness of 9 μm. (d) The effective
742 mean diameter of the fat aggregates, (e) the proportion of fat aggregates > 10 μm and (f) the
743 firmness of the cheeses at different pH.

744

745 Fig. 4. Schematic diagram illustrating the microstructure of standardized milk within which
746 the casein micelles (CM), fat globules (FG) with intact milk fat globule membrane (MFGM)
747 and whey protein are dispersed (a), the changes in the microstructure after milk
748 homogenization (inset showing the replacement of MFGM with CM and whey protein (WP))
749 (b), and the fermentation of the milk to higher pH (5.0) and lower gel pH (4.3-4.7), which lead
750 to different three dimensional gel networks (c). The heat treatment and whey separation lead
751 to compact gel particles (d). Further heating and curd texturizing leads to the formation of

752 cream cheese (e), which consists of corpuscular structures that are larger at higher pH than
753 at lower pH, dispersed gum that binds free serum within the structure and free fat. Fat is
754 illustrated in red, protein in green and whey protein as blue dots.
755
756 Fig. 5. S-FTIR analysis of cream cheese showing the average normalised absorbance (a)
757 and their corresponding second derivative (b1) spectra extracted from the areas of high
758 protein to lipid ratio, as determined by HCA. The broken line in (b1) indicates the range of
759 the amide I region (1600-1700 cm^{-1}) used for the plot in (b2). FTIR spectral maps of amide I
760 bands showing the spatial distribution of protein secondary structures including β-sheet and
761 β-turn as a function of cream cheese pH (c). Red indicates a high concentration of the
762 structure and dark blue indicates a low concentration, as indicated by the colour intensity
763 scale on the right. Representative images were selected for each pH treatment. The scale
764 bars are each 20 μm in length.
765
766 Fig. 6. PCA scores (a, c) and loading plots (b, d) obtained using second derivative spectra
767 extracted from areas containing high protein in the cream cheese samples with varying pH.
768 (a) Spectral range between 3000-2800 cm^{-1} and 1800-1100 cm^{-1} and (b) spectral range
769 within the amide I region (1700-1600 cm^{-1}).

Figure 1

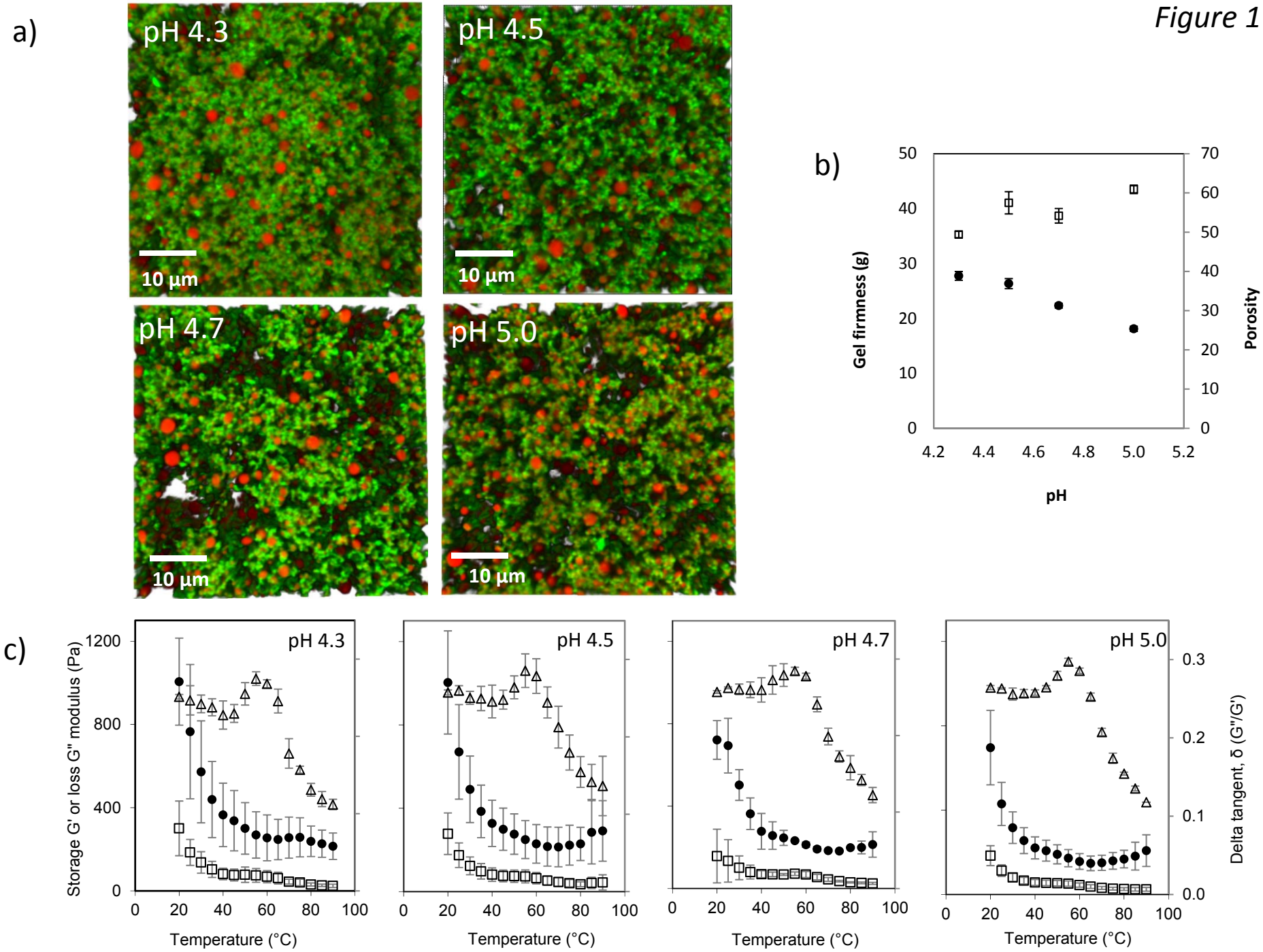
a)
pH 4.3
pH 4.5
pH 4.7
pH 5.0
10 µm
b)
Gel firmness (g)
Porosity
pH
c)
Storage G' or loss G'' modulus (Pa)
Delta tangent, δ (G''/G')
Temperature (°C)

Figure 2

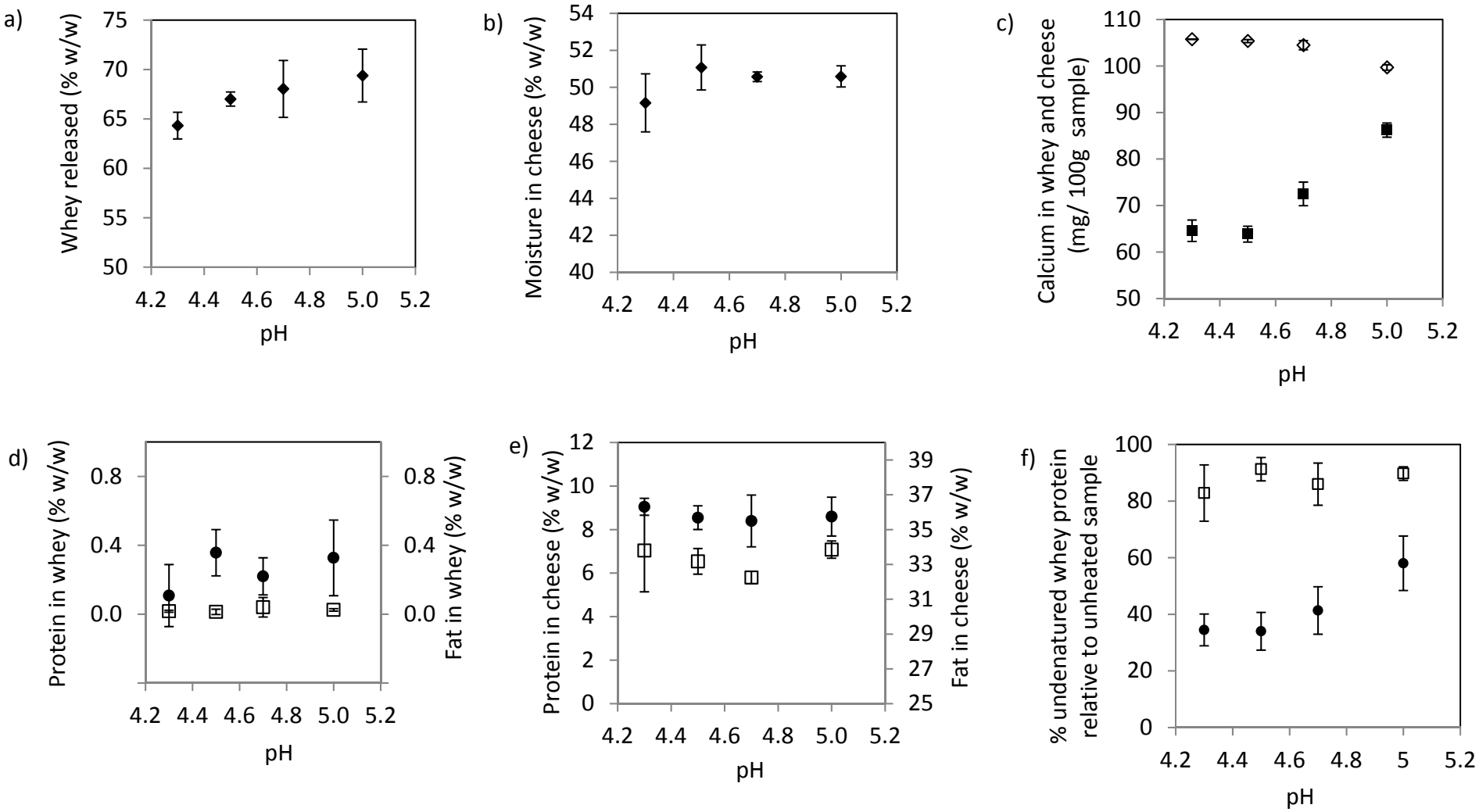
a)
Whey released (% w/w)
75
70
65
60
55
50
4.2 4.4 4.6 4.8 5.0 5.2
pH
b)
Moisture in cheese (% w/w)
54
52
50
48
46
44
42
40
4.2 4.4 4.6 4.8 5.0 5.2
pH
c)
Calcium in whey and cheese (mg/ 100g sample)
110
100
90
80
70
60
50
4.2 4.4 4.6 4.8 5.0 5.2
pH
d)
Protein in whey (% w/w)
Fat in whey (% w/w)
0.8
0.4
0.0
4.2 4.4 4.6 4.8 5.0 5.2
pH
e)
Protein in cheese (% w/w)
Fat in cheese (% w/w)
12
10
8
6
4
2
0
39
37
35
33
31
29
27
25
4.2 4.4 4.6 4.8 5.0 5.2
pH
f)
% undenatured whey protein relative to unheated sample
100
80
60
40
20
0
4.2 4.4 4.6 4.8 5 5.2
pH

Figure 3

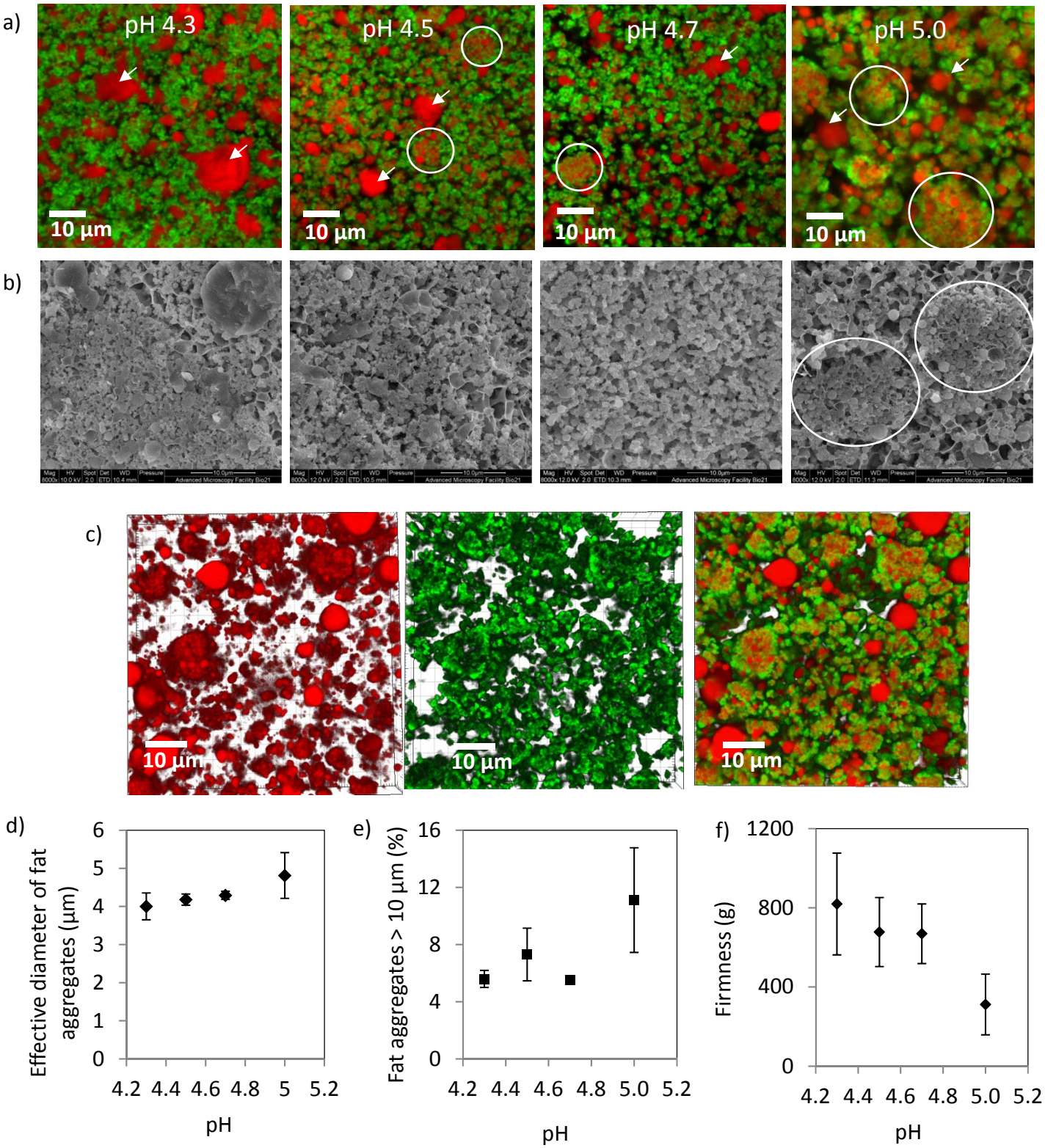
a)
pH 4.3
pH 4.5
pH 4.7
pH 5.0
10 µm
10 µm
10 µm
10 µm
b)
c)
10 µm
10 µm
10 µm
d)
Effective diameter of fat aggregates (µm)
0
1
2
3
4
5
6
4.2 4.4 4.6 4.8 5 5.2
pH
e)
Fat aggregates > 10 µm (%)
0
4
8
12
16
4.2 4.4 4.6 4.8 5.0 5.2
pH
f)
Firmness (g)
0
400
800
1200
4.2 4.4 4.6 4.8 5.0 5.2
pH

Figure 4

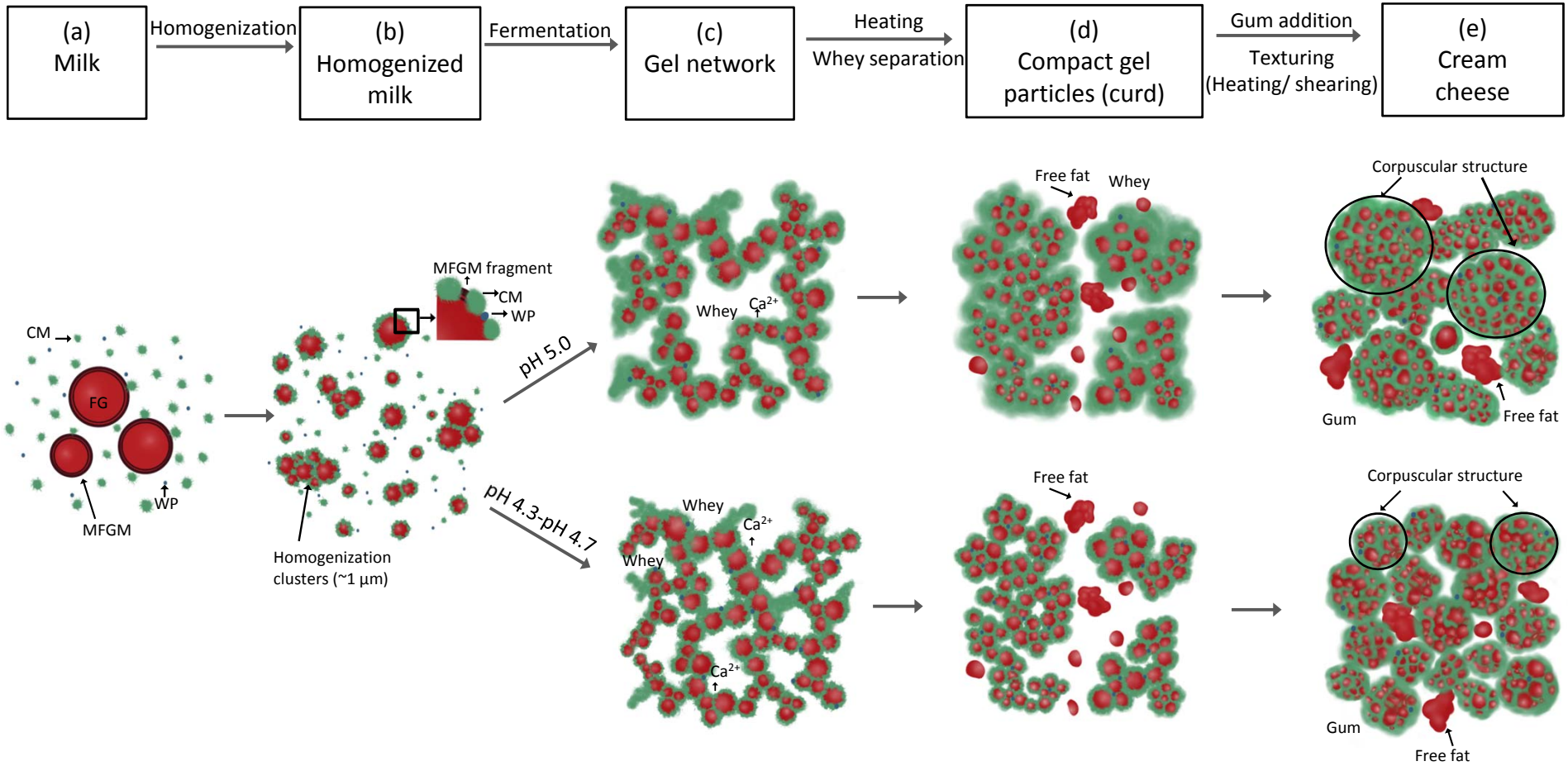
(a) Milk
Homogenization
(b) Homogenized milk
Fermentation
(c) Gel network
Heating
Whey separation
(d) Compact gel particles (curd)
Gum addition
Texturing (Heating/ shearing)
(e) Cream cheese
CM
FG
WP
MFGM
Homogenization clusters (~1 µm)
MFGM fragment
CM
WP
pH 5.0
pH 4.3-pH 4.7
Whey
Ca2+
Free fat
Whey
Corpuscular structure
Gum
Free fat

Figure 5

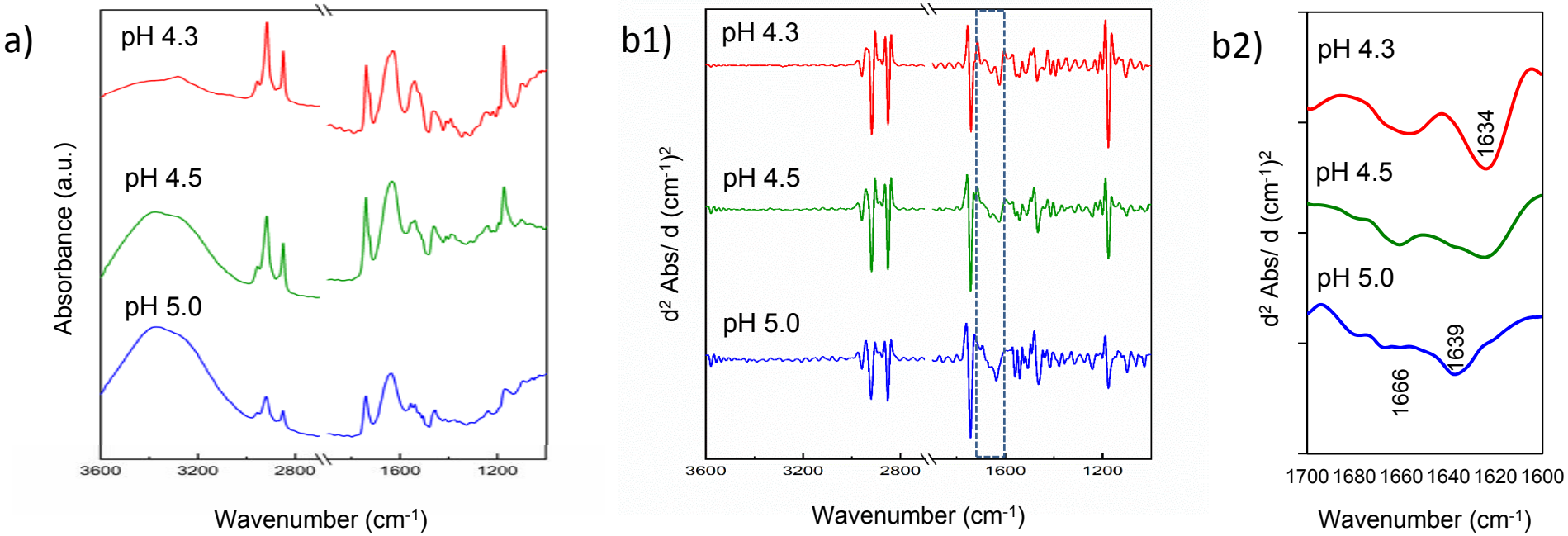
a)
pH 4.3
pH 4.5
pH 5.0
Absorbance (a.u.)
3600
3200
2800
1600
1200
Wavenumber (cm-1)
b1)
pH 4.3
pH 4.5
pH 5.0
d2 Abs/ d (cm-1)2
3600
3200
2800
1600
1200
Wavenumber (cm-1)
b2)
pH 4.3
pH 4.5
pH 5.0
1634
1639
1666
d2 Abs/ d (cm-1)2
1700 1680 1660 1640 1620 1600
Wavenumber (cm-1)

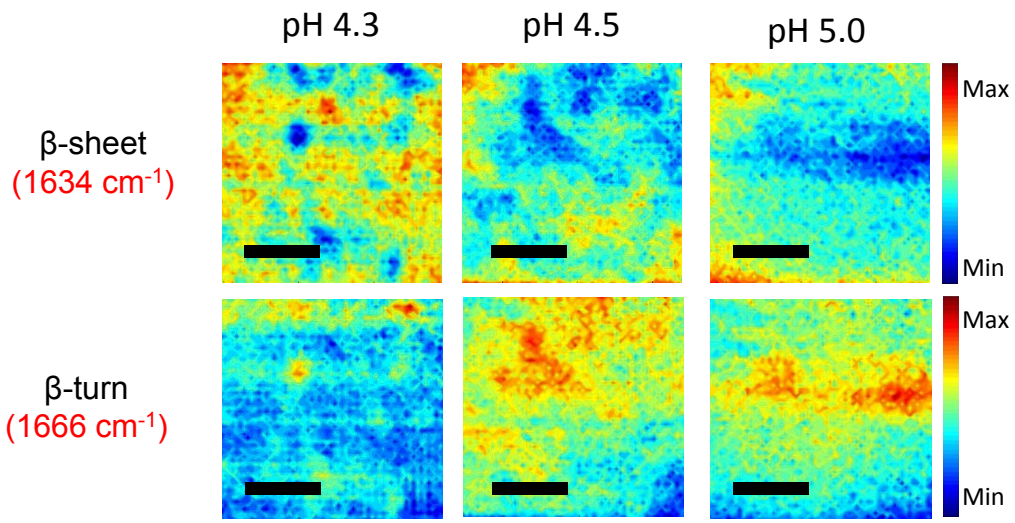
c)
pH 4.3
pH 4.5
pH 5.0
β-sheet
(1634 cm-1)
β-turn
(1666 cm-1)
Max
Min
Max
Min

Figure 6

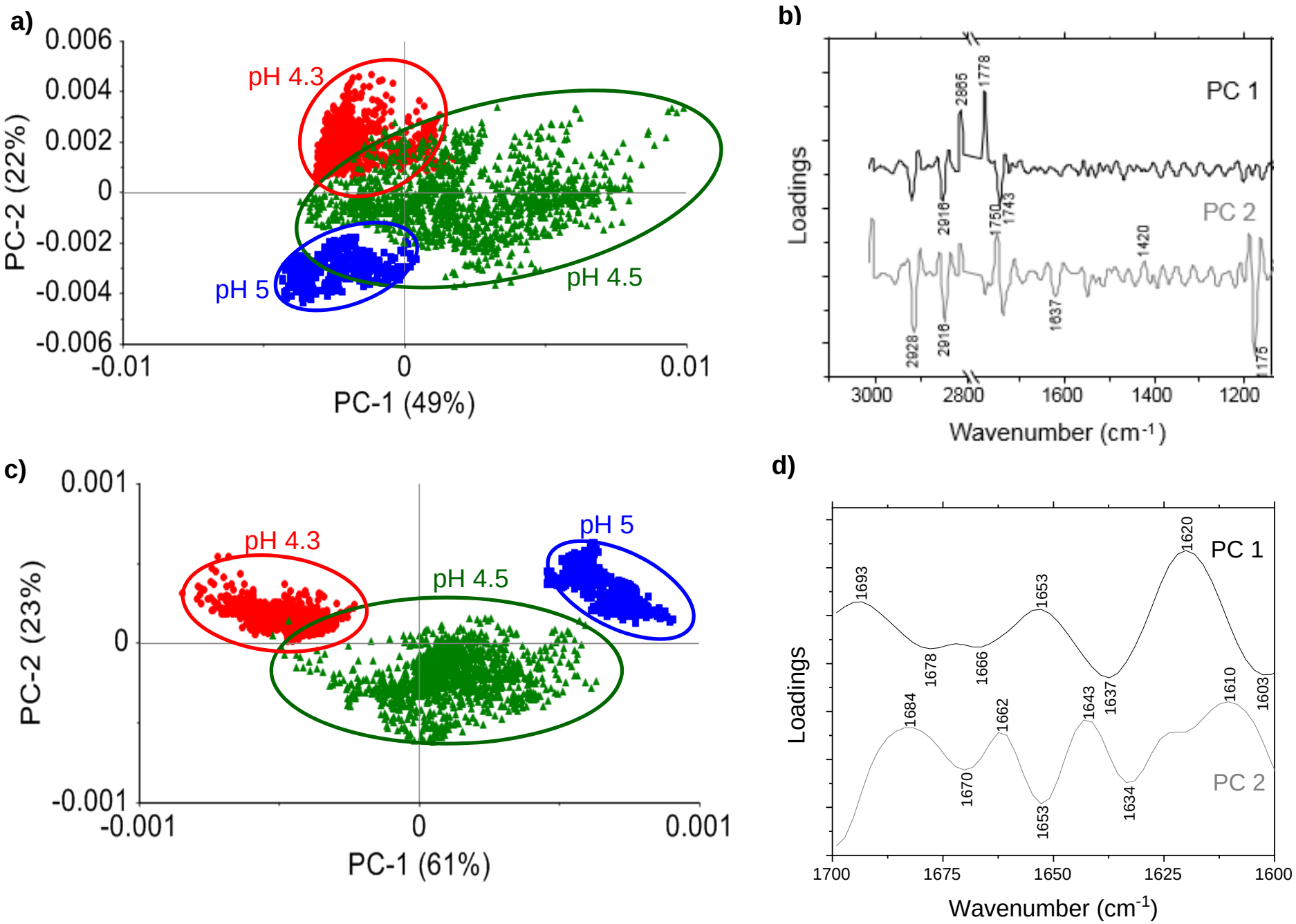
a)
pH 4.3
pH 5
pH 4.5
PC-2 (22%)
PC-1 (49%)
0.006
0.004
0.002
0
-0.002
-0.004
-0.006
-0.01
0
0.01
b)
PC 1
PC 2
Loadings
2885
1778
2918
1750
1743
1420
1637
2928
2918
1175
3000
2800
1600
1400
1200
Wavenumber (cm-1)
c)
pH 4.3
pH 5
pH 4.5
PC-2 (23%)
PC-1 (61%)
0.001
0
-0.001
-0.001
0
0.001
d)
PC 1
PC 2
Loadings
1693
1678
1666
1653
1637
1620
1610
1603
1684
1670
1662
1653
1643
1634
1700
1675
1650
1625
1600
Wavenumber (cm-1)